Lumped-parameter Model of a Bucket Foundation

Andersen, Lars; Ibsen, Lars Bo; Liingaard, Morten

Published in:
Computational Geomechanics : COMGEO I

Publication date:
2009

Document Version
Publisher's PDF, also known as Version of record

LUMPED-PARAMETER MODEL OF A BUCKET FOUNDATION

L. Andersen & L.B. Ibsen
Department of Civil Engineering, Aalborg University, Denmark

M.A. Liingaard
DONG Energy A/S, Fredericia, Denmark

ABSTRACT: *As an alternative to gravity footings or pile foundations, offshore wind turbines at shallow water can be placed on a bucket foundation. The present analysis concerns the development of consistent lumped-parameter models for this type of foundation. The aim is to formulate a computationally efficient model that can be applied in aero-elastic codes for fast evaluation of the dynamic structural response of wind turbines. The target solutions, utilised for calibration of the lumped-parameter models, are obtained by a coupled finite-element/boundary-element scheme in the frequency domain, and the quality of the models are tested in the time and frequency domains. It is found that precise results are achieved by lumped-parameter models with two to four internal degrees of freedom per displacement or rotation of the foundation. Further, coupling between the horizontal sliding and rocking cannot be disregarded without significant loss of accuracy. Finally, special attention is drawn to the influence of the skirt stiffness, i.e. whether the embedded part of the caisson is rigid or flexible.*

1 INTRODUCTION

The design of modern wind turbines is to a great extent based on numerical simulation by means of aero-elastic codes, e.g. FAST (Jonkman & Buhl 2005). An accurate prediction of the structural response requires a model that accounts for the dynamic soil-structure interaction. Since computational speed is of paramount importance, e.g. for the evaluation of the fatigue life, only few degrees of freedom should be associated with the model of the foundation and the subsoil. For this purpose, a lumped-parameter model fitted to the results of a rigorous model is useful (Wolf & Paronesso 1992; Andersen & Liingaard 2007; Andersen 2008).

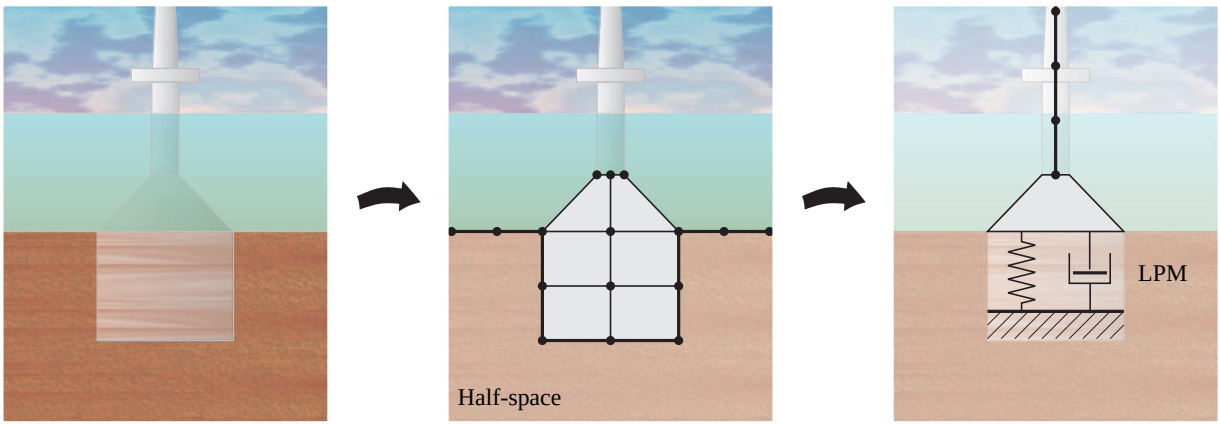

Fig. 1. Bucket foundation in homogeneous soil (left); finite-element/boundary-element model of the foundation and the subsoil (centre); lumped-parameter model of the foundation coupled with a finite-element model of the structure (right).

This paper focuses on the development of consistent lumped-parameter models (LPMs) for steel suction caissons that may be applied as foundations for offshore wind turbines on shallow water. Presently, a single offshore wind turbine has been installed on a bucket foundation in Frederikshavn, Denmark (Ibsen 2008). The turbine has been in operation since 2002. Since the suction bucket is applied as a monopod, it carries loads and moments in all directions. Further, due to the embedment of the skirted foundation, a significant coupling exists between these degrees of freedom. Such coupling has been analysed by, for example, Veletsos & Wei (1971) or Bu & Lin (1999). Hence, a lumped-parameter model of a bucket foundation must account for the sliding–rocking coupling in contrast to the case of a surface footing on a homogeneous or layered ground, where the coupling is often negligible (Andersen 2008).

In Section 2 the theory is shortly outlined, following the overall concept illustrated in Fig. 1. Firstly, the dynamic flexibility of a bucket foundation embedded in homogeneous soil is computed, employing a three-dimensional coupled finite-element/boundary-element scheme in the frequency domain (Andersen & Jones 2001). The number of discrete frequencies is sufficiently high to capture the local variations in the stiffness due to constructive and destructive interference of waves inside the bucket. Secondly, a consistent LPM is fitted for each degree of freedom of the foundation, i.e. heave, torsion, horizontal sliding and rocking. In addition to this, an LPM is established for the sliding–rocking coupling terms. Thirdly, in Section 3 the quality of the LPMs is tested in the frequency and time domains. It is shown that accurate results are achieved when LPMs with approximately three internal degrees of freedom are applied for each component of the dynamic stiffness. Finally, the main conclusions are summarised in Section 4.

2 COMPUTATIONAL MODEL OF THE BUCKET FOUNDATION

A rigid footing has three translational and three rotational degrees of freedom, see Fig. 2. In the frequency domain, these are related to the complex amplitudes of the forces and moments as

$$\mathbf{CZ} = \mathbf{F}, \quad \mathbf{Z} = \begin{bmatrix} V_1 \\ V_2 \\ V_3 \\ \Theta_1 \\ \Theta_2 \\ \Theta_3 \end{bmatrix}, \quad \mathbf{F} = \begin{bmatrix} Q_1 \\ Q_2 \\ Q_3 \\ M_1 \\ M_2 \\ M_3 \end{bmatrix}, \quad \mathbf{C} = \begin{bmatrix} C_{22} & 0 & 0 & 0 & -C_{24} & 0 \\ 0 & C_{22} & 0 & C_{24} & 0 & 0 \\ 0 & 0 & C_{33} & 0 & 0 & 0 \\ 0 & C_{24} & 0 & C_{44} & 0 & 0 \\ -C_{24} & 0 & 0 & 0 & C_{44} & 0 \\ 0 & 0 & 0 & 0 & 0 & C_{66} \end{bmatrix}. \quad (1)$$

Here $\mathbf{Z} = \mathbf{Z}(\omega)$ stores the amplitudes of the displacements and rotations, whereas $\mathbf{F} = \mathbf{F}(\omega)$ is the vector of forces and moments acting on the rigid footing with ω denoting the circular frequency of excitation. In the general case, the impedance matrix $\mathbf{C} = \mathbf{C}(\omega)$ is fully populated, i.e. all the rigid-body motions of the footing are interrelated. However, due to the axial symmetry in the present case, $C_{11} = C_{22}$, $C_{44} = C_{55}$ and $C_{15} = -C_{24}$.

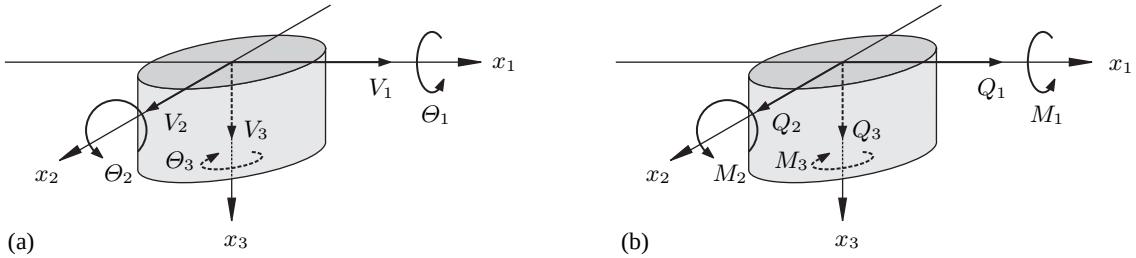

Fig. 2. Degrees of freedom for a rigid footing: (a) displacements and rotations; (b) forces and moments.

Furthermore, torsion and heave are completely decoupled from sliding and rocking, and the sliding in the x_1-direction is only coupled with the rocking about the x_2-axis (and vice versa).

2.1 Coupled boundary-element/finite-element model in the frequency domain

In the present analysis, a bucket foundation with the radius $r_0 = 8$ m, the skirt length $h_0 = 8$ m and the skirt thickness $t_0 = 50$ mm is considered (see Fig. 3). The impedance matrix $\mathbf{C}(\omega)$ is evaluated at a number of discrete frequencies, based on the computations carried out by a coupled finite-element/boundary-element (FE/BE) model. The materials are assumed to be linear viscoelastic, employing a hysteretic damping model, i.e. the material dissipation is independent of the frequency. Hence, each material is defined by the Young's modulus E, the Poisson's ratio ν, the mass density ρ, and the loss factor η.

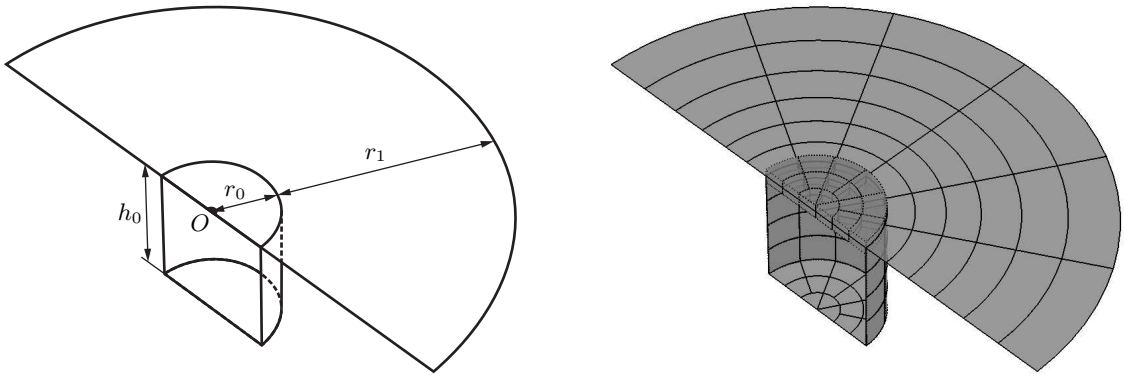

Fig. 3. Coupled finite-element/boundary-element model of skirted foundation: Geometry (left) and discretization (right). Only half of the foundation is discretized, utilising the symmetry of the problem.

Isoparametric shell finite elements with quadratic Lagrangian interpolation of the rotation and displacement of the mid-plane are employed for the foundation (Cook et al. 2002). Shear deformation over the thickness direction is allowed in accordance with the Mindlin-Reissner assumption. The lid of the bucket is assumed to be relatively stiff, modelled as a 1 m thick, massless plate of the material denoted "rigid" in Table 1. The skirts are assumed to be massless and rigid, made by the same material as the lid, or they consist of massless steel. The mass of the skirts has almost no impact on the impedance of the foundation, whereas the flexibility (i.e. Young's modulus) has a significant effect on the response as further discussed in Section 3.

The material properties of the soil are listed in Table 1. The P-wave velocity is about 436 m/s and the S-wave speed is approximately 131 m/s, corresponding to soft sand in drained conditions. For the subsoil, quadrilateral boundary elements with quadratic Lagrangian interpolation of the displacement and the surface traction are applied (Domínguez 1993). The full-space Green's function is employed, and therefore the surface of the half-space needs to be discretized. As illustrated in Fig. 3, the surface is truncated at the distance r_1 away from the foundation. In the present analyses, $r_1 = 32$ m has been found to ensure that the artificial boundary will not influence the response of the foundation significantly.

Table 1. Material properties of the massless bucket foundation and the subsoil used in the computations.

Material	E (MPa)	ν	ρ (kg/m^3)	η
Soil	100	0.45	2000	0.05
Bucket (steel)	$2 \cdot 10^5$	0.30	0	0.01
Bucket (rigid)	$2 \cdot 10^{10}$	0.30	0	0.01

To increase the computational efficiency, the symmetry of the problem has been utilised by modelling only half of the foundation and the surrounding half-space. The discretization is illustrated in Fig. 3 (right), where it is noted that the soil inside and outside the bucket have been modelled as two separate boundary-element domains. The complete model is obtained by transforming the boundary-element domains into equivalent macro finite elements that may, subsequently, be coupled with the finite-element model of the foundation. Details about the FE/BE model can be found in the previous work by Andersen & Jones (2001) and Andersen (2002).

At each frequency, the FE/BE model is subjected to a set of loads providing a vertical force, Q_3, a torsional moment, M_3, a horizontal force, Q_1 or a rocking moment, M_2. Example results are shown in Fig. 4 for a rocking moment applied at the frequencies 5 an 10 Hz. The displacements and the rotations of the lid are computed for each set of loads, leading to the components of a dynamic flexibility matrix for the foundation. This matrix is finally inverted to get the impedance matrix $\mathbf{C}(\omega)$. Due to discretization errors, the FE/BE model provides different values for C_{24} and C_{42}. The symmetry of $\mathbf{C}(\omega)$ is enforced by using the mean value $(C_{24} + C_{42})/2$.

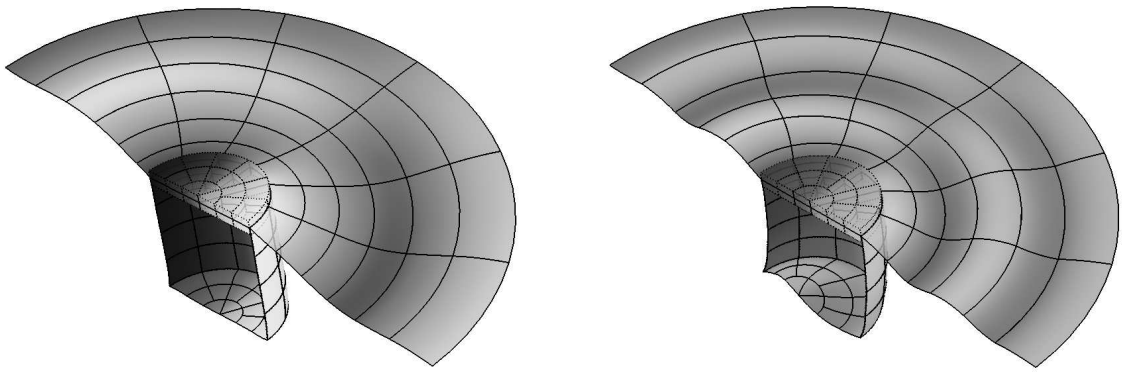

(a) (b)

Fig. 4. Response of the skirted foundation plotted 0.2 excitation period out of phase with the load: (a) Rocking moment of the magnitude $1 \cdot 10^{11}$ applied at the frequency $f = 5$ Hz; (b) rocking moment of the magnitude $3 \cdot 10^{11}$ applied at the frequency $f = 10$ Hz. The light and dark shades of grey indicate vertical displacements upwards and downwards, respectively.

2.2 Consistent lumped-parameter model for time-domain analysis

Component (i, j) of the impedance matrix may be expressed as $C_{ij}(\omega) = K_{ij}S_{ij}(\omega)$, where $K_{ij} = C_{ij}(0)$ is the static stiffness component and S_{ij} is the normalised dynamic stiffness. As proposed by Wolf (1994), the frequency-dependent stiffness is decomposed into a singular and a regular part. In terms of the normalised dynamic stiffness, and skipping indices i and j, each component may be written as

$$C(\omega) = KS(\omega), \qquad S(\omega) = S_s(\omega) + S_r(\omega). \tag{2}$$

Here, K is the static stiffness component, whereas $S_s(\omega)$ and $S_r(\omega)$ are the singular part and the regular part of $S(\omega)$, respectively. These are given as

$$S_s(\omega) = k^\infty + \mathrm{i}\omega c^\infty, \qquad S_r(\omega) \approx \hat{S}_r(\mathrm{i}\omega) = \frac{P(\mathrm{i}\omega)}{Q(\mathrm{i}\omega)}, \tag{3a}$$

where $\mathrm{i} = \sqrt{-1}$ is the imaginary unit, while $P(\mathrm{i}\omega)$ and $Q(\mathrm{i}\omega)$ are polynomials of the orders $M - 1$ and M, respectively, i.e.

$$P(\mathrm{i}\omega) = 1 - k^\infty + p_1(\mathrm{i}\omega) + p_2(\mathrm{i}\omega)^2 + \ldots + p_{M-1}(\mathrm{i}\omega)^{M-1}, \tag{3b}$$

$$Q(\mathrm{i}\omega) = 1 + q_1(\mathrm{i}\omega) + q_2(\mathrm{i}\omega)^2 + \ldots + q_M(\mathrm{i}\omega)^M. \tag{3c}$$

In Eq. (3) all coefficients are real. The rational approximation $\hat{S}_r(\mathrm{i}\omega) \to 0$ for $\omega \to \infty$, and $\hat{S}_r(0) = 1 - k^\infty$. Hence, the static stiffness is recovered for $\omega = 0$, and $KS_s(\omega)$ provides the entire dynamic stiffness in the high-frequency limit, leading to a double-asymptotic solution.

For a rigid footing, the term Kk^∞ vanishes and the singular part of the dynamic stiffness is reduced to a pure mechanical impedance. With ρ, c_P and c_S denoting the mass density, the P-wave speed and the S-wave speed of the soil, respectively, the high-frequency limit of the impedance related to the coupled sliding and rocking of a rigid bucket foundation are given as

$$c_{11}^\infty = c_{22}^\infty = \rho c_S A^{lid} + \frac{1}{2}\left(\rho c_S + \rho c_P\right) A^{skirt}, \tag{4a}$$

$$c_{24}^\infty = c_{42}^\infty = -\frac{1}{4}\left(\rho c_S + \rho c_P\right) h_0 A^{skirt} = -c_{15}^\infty = -c_{51}^\infty, \tag{4b}$$

$$c_{44}^\infty = c_{55}^\infty = \rho c_P \mathcal{I}^{lid} + \frac{1}{2}\left(\rho c_S + \rho c_P\right) \mathcal{I}^{skirt} + \frac{1}{2}\rho c_S r_0^2 A^{skirt}. \tag{4c}$$

$$c_{33}^\infty = \rho c_P A^{lid} + \rho c_S A^{skirt}, \qquad c_{66}^\infty = 2\rho c_S \mathcal{I}^{lid} + \rho c_S r_0^2 A^{skirt}, \tag{4d}$$

The areas and the geometrical moments of inertia around the centroid of the lid are given as

$$A^{lid} = \pi r_0^2, \qquad A^{skirt} = 4\pi r_0 h_0, \qquad \mathcal{I}^{lid} = \frac{\pi}{4} r_0^4, \qquad \mathcal{I}^{skirt} = \frac{4\pi}{3} r_0 h_0^3. \tag{4e}$$

The contributions from both sides of the skirt are included in A^{skirt} and $\mathcal{I}^{skirt}$.

Equation (4) may provide an overestimation of the high-frequency impedance of a flexible foundation. Alternatively a solution with no contributions from the skirt may be proposed, or the skirt may be treated as a part of the subsoil. In the latter case, the coupling between sliding and rocking vanishes in the high-frequency limit, i.e. $c_{24}^\infty = c_{42}^\infty = c_{15}^\infty = c_{51}^\infty = 0$, and

$$c_{11}^\infty = c_{22}^\infty = \rho c_S A^{lid} + \rho^{skirt} c_S^{skirt} A^{ring}, \qquad c_{33}^\infty = \rho c_P A^{lid} + \rho^{skirt} c_P^{skirt} A^{ring}, \tag{5a}$$

$$c_{44}^\infty = c_{55}^\infty = \rho c_P \mathcal{I}^{lid} + \rho^{skirt} c_P^{skirt} \mathcal{I}^{ring}, \qquad c_{66}^\infty = 2\rho c_S \mathcal{I}^{lid} + 2\rho^{skirt} c_S^{skirt} \mathcal{I}^{ring}, \tag{5b}$$

where ρ^{skirt}, c_P^{skirt} and c_S^{skirt} are the mass density, the P-wave speed and the S-wave speed of the skirt material, respectively. Further, $A^{ring} \approx 2\pi t_0$ and $\mathcal{I}^{ring} \approx \pi t_0 r_0^3$ are the area and the geometrical moment of inertia around the centroid related to the horizontal cross section of the skirt. Selecting a proper value of the high-frequency impedance components is crucial to obtaining a well-posed lumped-parameter model as discussed in the next section.

Regarding the regular part of the non-dimensional dynamic stiffness, $S_r(\omega)$, the order M of the rational approximation, $\hat{S}_r(\mathrm{i}\omega)$, must be high enough to ensure an accurate fit to the target solution, obtained by the FE/BE scheme, and low enough to avoid wiggling outside the range of frequencies considered in the FE/BE model. Furthermore, to provide a physically valid solution the poles of the rational approximation, i.e. the roots of the denominator polynomial, must all have a negative real part. In particular, if there are N complex conjugate pairs of poles, $Q(\mathrm{i}\omega)$ may advantageously be written as

$$Q(\mathrm{i}\omega) = \prod_{n=1}^{N} \left(\mathrm{i}\omega - s_n\right)\left(\mathrm{i}\omega - s_n^*\right) \cdot \prod_{n=N+1}^{M-N} \left(\mathrm{i}\omega - s_n\right). \tag{6}$$

where s_n, $n = 1, 2, \ldots, N$, are complex roots with s_n^* defining their complex conjugates. The remaining $M - 2N$ roots are real.

The rational approximation $\hat{S}_r(\mathrm{i}\omega)$ is now fitted to the target solution $S_r(\mathrm{i}\omega)$ computed by the FE/BE model at the circular frequencies ω_j, $j = 1, 2, \ldots, J$, employing a weighted least squares approach with the weight function $w(\omega)$. The polynomial coefficients p_n and the poles s_m are identified as the optimisation variables. Hence, the object function

$$F(p_n, s_m) = \sum_{j=1}^{J} w(\omega_j) \left(\hat{S}_r(\mathrm{i}\omega_j) - S_r(\omega_j) \right)^2 \tag{7}$$

is minimised subject to one equality constraint,

$$G_0 = 1 - \prod_{n=1}^{N} (s_n) \, (s_n^*) \cdot \prod_{n=N+1}^{M-N} (-s_n) = 0, \tag{8a}$$

and M inequality constraints,

$$G_k = \Re(s_k) + \varepsilon < 0, \qquad k = 1, 2, \ldots, N, \tag{8b}$$

$$G_k = s_k + \varepsilon < 0, \qquad k = N+1, 2, \ldots, M-N, \tag{8c}$$

$$G_j = \zeta \Re(s_k) + \Im(s_k) < 0, \qquad j = M - N + k, \qquad k = 1, 2, \ldots, N. \tag{8d}$$

Here, $\Re(s_k)$ and $\Im(s_k)$ are the real and imaginary parts of the complex conjugate poles, respectively. Further, $\zeta \approx 10 - 100$ and $\varepsilon \approx 0.01$ are two real parameters introduced to avoid errors due to limited computational accuracy. The equality constraint ensures that $\hat{S}_r(0) = 0$ in accordance with Eq. (3c), whereas the third inequality constraint guaranties that the complex first-order poles will not form non-negative real second-order poles. As suggested by Wolf (1994) and Andersen (2008), the weight function $w(\omega)$ is designed as a decreasing function of the frequency, which ensures a good match at low frequencies. Obviously, the initial values of the poles must conform with the constraint $G_0 = 0$.

The polynomial-fraction form of the rational approximation, given by Eq. (3), is recast into a partial-fraction form. With N complex conjugate pairs of poles in $\hat{S}_r(\mathrm{i}a_0)$, the total approximation of the dynamic stiffness coefficient $S(a_0)$ can be written as

$$\hat{S}(\mathrm{i}a_0) = k^\infty + \mathrm{i}a_0 c^\infty + \sum_{n=1}^{N} \frac{\beta_{0n} + \beta_{1n}\mathrm{i}a_0}{\alpha_{0n} + \alpha_{1n}\mathrm{i}a_0 + (\mathrm{i}a_0)^2} + \sum_{n=N+1}^{M-N} \frac{A_n}{\mathrm{i}a_0 - s_n}. \tag{9a}$$

Here A_n are the residues corresponding to the real poles s_n, $n = N+1, N+2, \ldots, M-N$. The real coefficients α_{0n}, α_{1n}, β_{0n}, and β_{1n} are given by

$$\alpha_{0n} = \{\Re(s_n)\}^2 + \{\Im(s_n)\}^2, \qquad \alpha_{1n} = -2\Re(s_n), \tag{9b}$$

$$\beta_{0n} = -2\Re(A_n)\Re(s_n) + 2\Im(A_n)\Im(s_n), \qquad \beta_{1n} = 2\Re(A_n), \tag{9c}$$

where $\Re(A_n)$ and $\Im(A_n)$ are the real and imaginary parts of the complex conjugate residues.

The total approximation of the dynamic stiffness given by Eq. (9) consists of three characteristic types of terms, namely a constant/linear term, $M - 2N$ first-order terms and N second-order terms. Each of these expressions may be interpreted as the frequency-response function for a so-called discrete-element model as illustrated in Fig. 5. The spring and damping coefficients as well as the point masses in these models are uniquely defined in terms of the coefficients in Eq. (9). A detailed explanation may be found, for example, in the work by Wolf (1994) or Liingaard (2006). Here, it shall only be noted that the optimal solution includes as many complex conjugate pairs as possible modelled by the alternative second-order system, cf. Fig. 5e, since this reduces the number of internal degrees of freedom in the resulting lumped-parameter model (LPM) to a minimum for a given order, M, of the rational approximation.

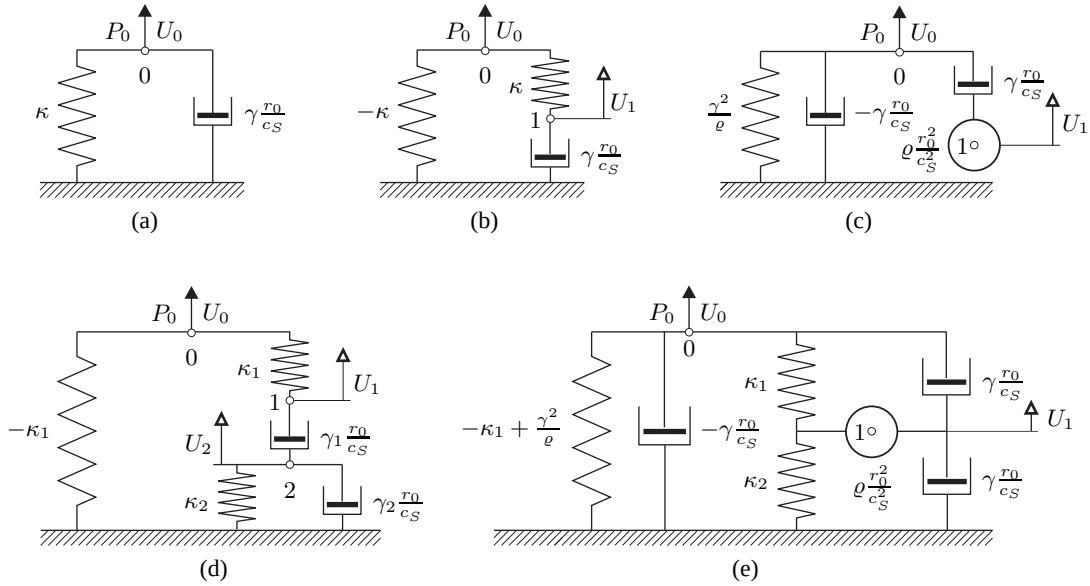

Fig. 5. Discrete-element models: (a) Constant/linear term; (b) standard first-order term; (c) alternative first-order term, also known as a "monkey tail"; (d) standard second-order term (two internal degrees of freedom); (e) alternative second-order term.

3 RESULTS AND DISCUSSION

A bucket foundation with the geometry described in Subsection 2.1 is analysed in the frequency domain by a coupled FE/BE model. The target solution is computed at the discrete frequencies $f = 0, 0.1, 0.2, \ldots, 20$ Hz for two cases: a bucket foundation with rigid skirts and a bucket foundation with skirts made by steel. In both cases, the skirts are assumed to be massless, but it has been tested that the mass of the skirts has almost no impact on the overall response. As outlined in Subsection 2.2, lumped-parameter models are fitted to the target solutions. The LPMs are tested in the time domain by comparing the response to a transient load with the results obtained by inverse Fourier transformation of the target solution carried out in the frequency domain.

3.1 A bucket foundation with rigid skirts

Based on the results of FE/BE analysis for the foundation with rigid skirts, the target solutions $S_{33}(\omega), S_{22}(\omega)$, etc. have been computed. Figure 6 shows the results in terms of the magnitudes $|S_{33}|, |S_{22}|$, etc. and the phase angles $\arg(S_{33}), \arg(S_{22})$, etc. and as functions of the frequency, f. Note that only one out of ten data has been included in the figure, but evidently the local tips and dips occurring due to interference of waves inside the bucket are well represented.

As indicated by Fig. 6, the FE/BE model provides results that oscillate around the singular part of the normalised dynamic stiffness, computed by Eq. (4) for the rigid bucket. Moreover, lumped-parameter models if the order $M = 4$ can be used at frequencies below approximately 2 Hz for the present foundation and subsoil. At higher frequencies, up to about 5–10 Hz, an LPM of the order $M = 8$ is valid. Utilising the discrete-element model illustrated in Fig. 5e, four internal degrees of freedom are added for each non-zero component of the impedance matrix, $\mathbf{C}(\omega)$. It is noted that the off-diagonal terms representing the coupling between sliding and rocking (and vice versa) must be considered separate quantities in the development of LPMs—even though the impedance matrix is symmetric. Hence, a great reduction in the total size of the model can be achieved if the coupling may be disregarded.

The quality of the lumped-parameter models of the orders $M = 4$ and 8 are tested in the time domain by application of a transient load. The time histories of the load and the response

are given in Fig. 7, where $q_3(t)$ is a vertical force applied at the centre of the lid and $v_3(t)$ is the vertical displacement of the lid. Likewise, $\theta_3(t)$ is the torsional rotation due to the torsional moment $M_3(t)$, and so on. A rigid cylinder with a mass density of 2000 kg/m^3, a radius of $r_0 = 8$ m and a height of 32 m has been put on top of the foundation, and the response has been integrated over time. For the present time-history of the excitation, both LPMs provide useful

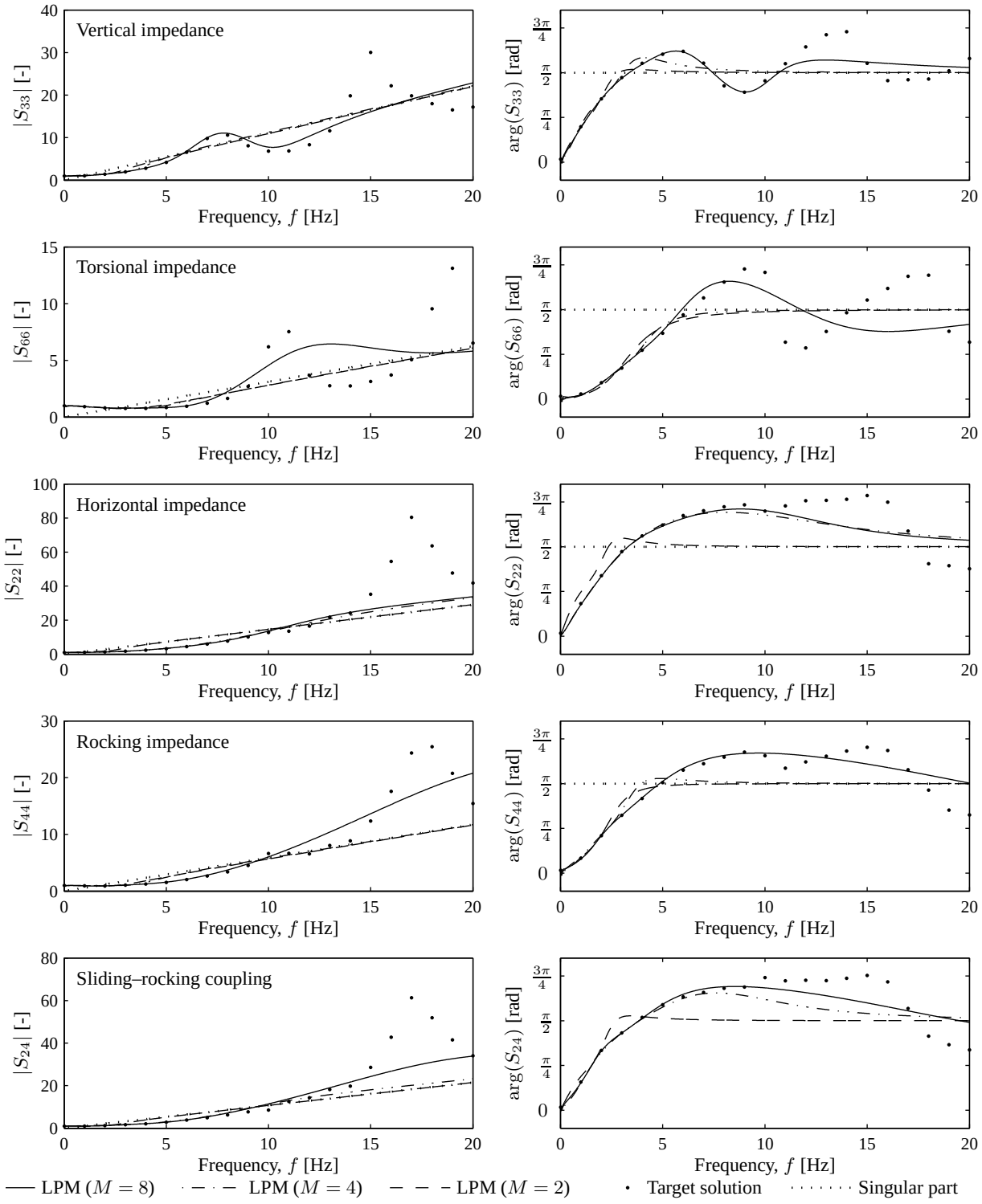

Fig. 6. Dynamic stiffness coefficients for the bucket foundation with rigid skirts obtained by the FE/BE model (target solution) and lumped-parameter models with different orders.

results, i.e. the responses provided by the LPMs are in good agreement with the results achieved by inverse Fourier transformation of the frequency-domain solutions based on the FE/BE model. The approximation of the order $M = 8$ is slightly more accurate regarding the prediction of the maximum response during the application of the load as well as the geometrical damping occurring after the excitation has ended. Clearly, sliding–rocking coupling cannot be disregarded.

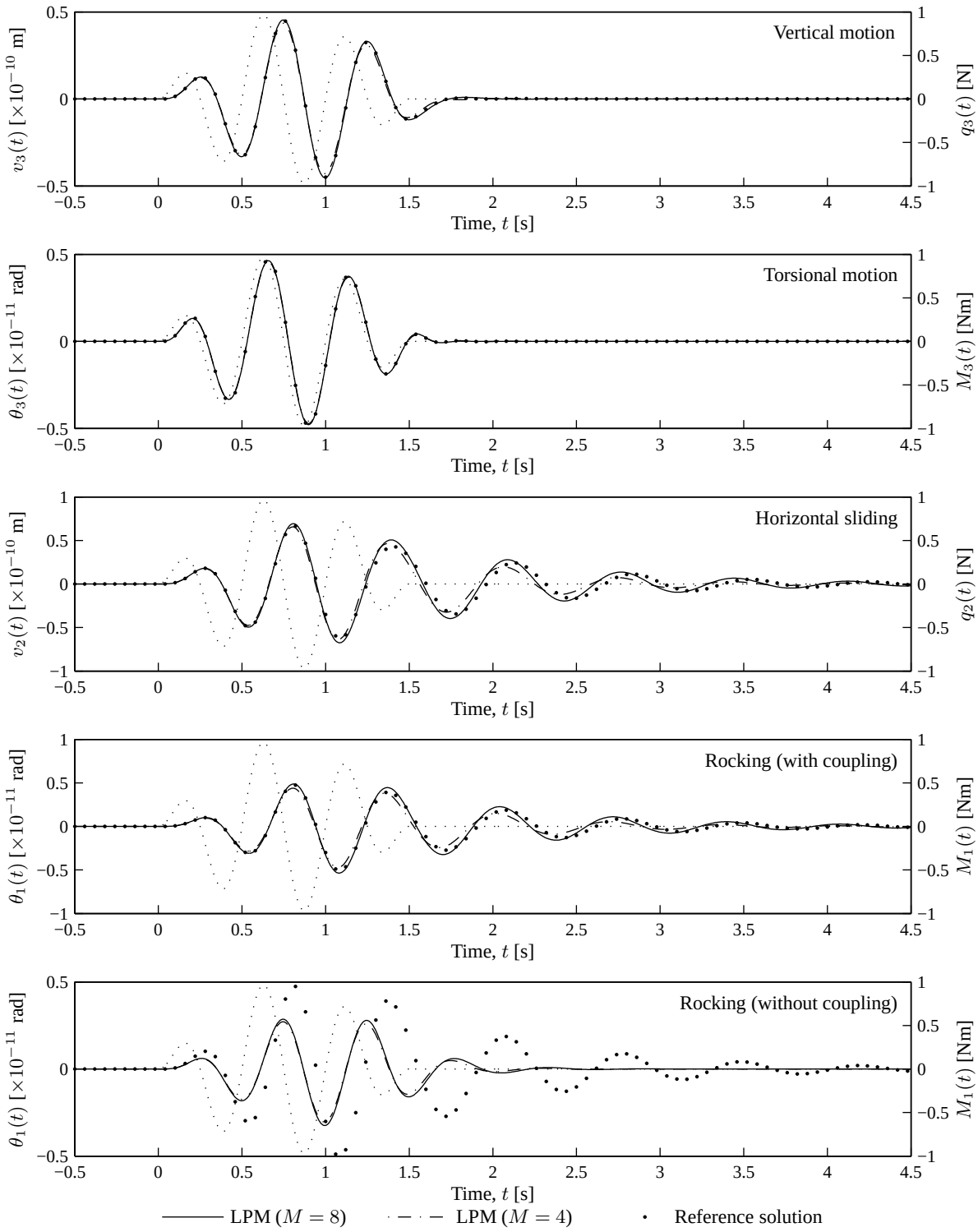

Fig. 7. Response of the bucket foundation with rigid skirts obtained by inverse Fourier transformation (reference solution) and lumped-parameter models. The dots indicate the load time history.

3.2 A bucket foundation with flexible skirts

Similarly to the previous analysis of a rigid bucket foundation, lumped-parameter models are established for a bucket foundation with flexible skirts with a stiffness corresponding to that of steel. The frequency-domain and time-domain results are given in Figs. 8 and 9, respectively. Again, a good match to the target solution is obtained with LPMs of the order $M = 4$ to $M = 8$.

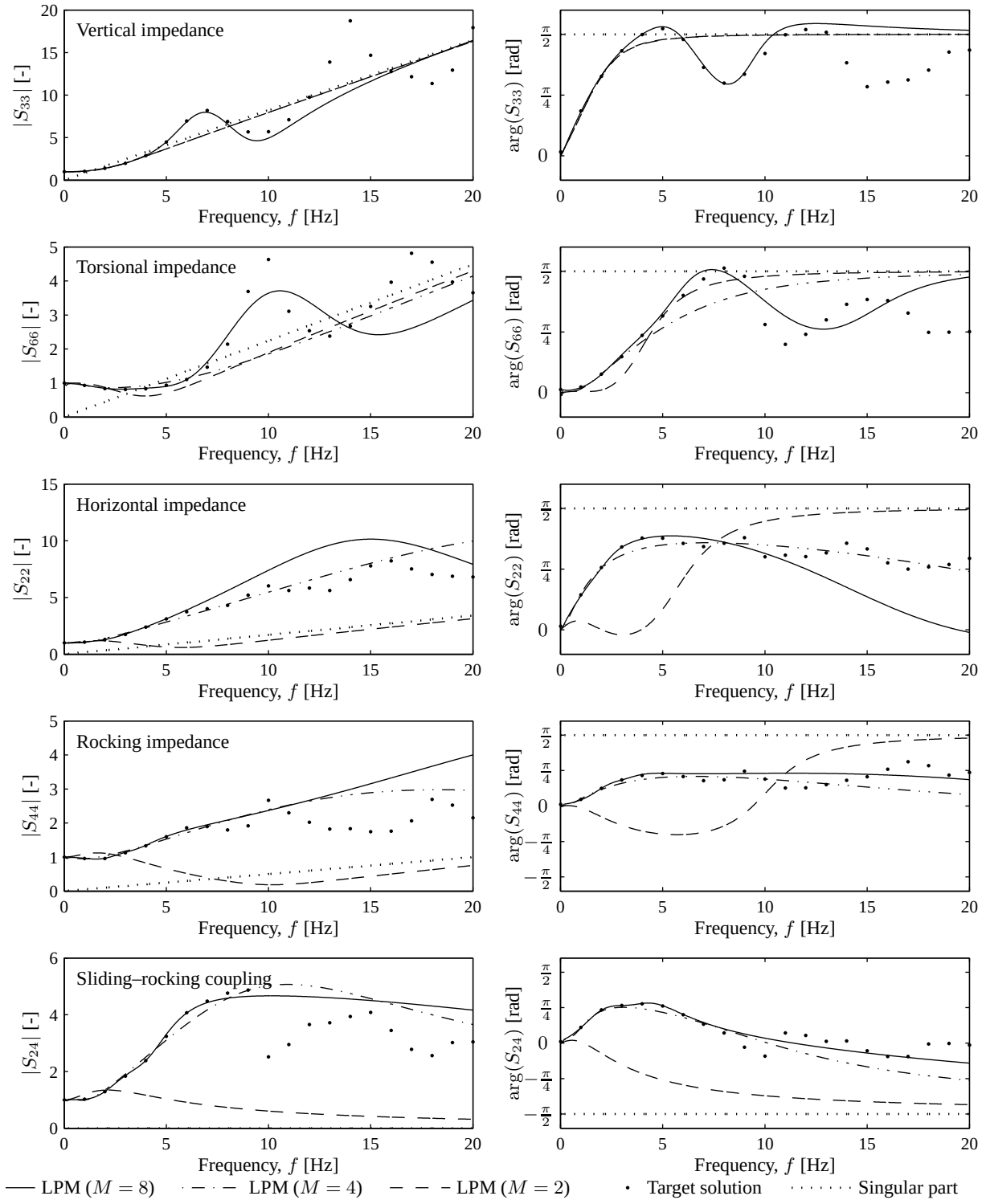

Fig. 8. Dynamic stiffness coefficients for the bucket foundation with flexible skirts obtained by the FE/BE model (target solution) and lumped-parameter models with different orders.

It is noted that the singular parts given by Eq. (5) have been applied for the sliding and rocking degrees of freedom, including the coupling terms. However, for the heave and the torsion, a mix with half the impedances defined by Eq. (4) and half the impedances given by Eq. (5) has been found to provide a good approximation in the high-frequency domain. Even if the sliding-rocking coupling is weaker than in the case of the rigid footing, it cannot be disregarded.

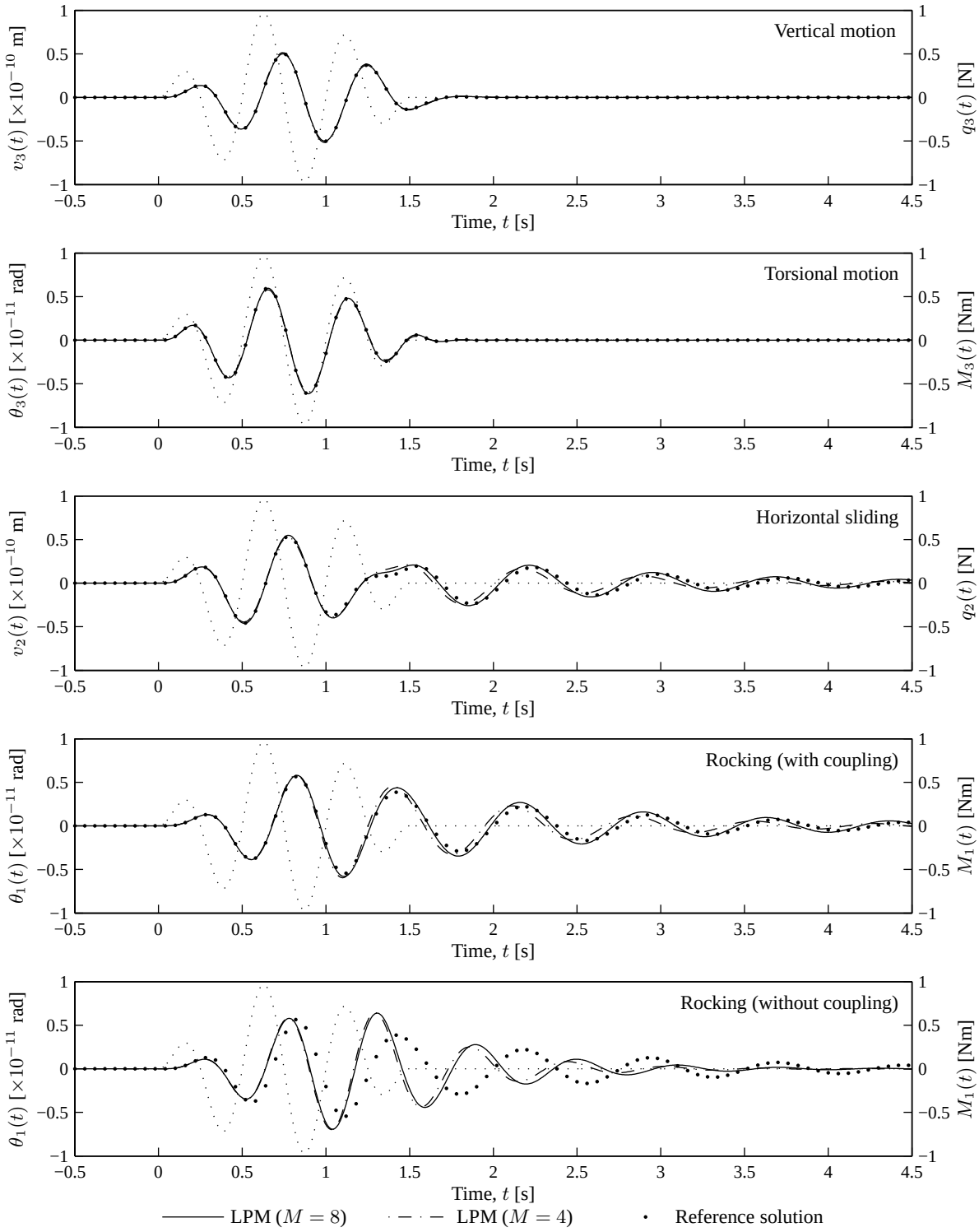

Fig. 9. Response of the bucket foundation with flexible skirts obtained by inverse Fourier transformation (reference solution) and lumped-parameter models. The dots indicate the load time history.

4 CONCLUSION

Consistent lumped-parameter models have been devised for rigid as well as flexible bucket foundations situated in homogeneous soil. It has been found that rational approximations of the order 4 to 8 provide useful results at frequencies below 2 to 10 Hz. Hence, models with about 3 internal degrees of freedom per non-zero component of the impedance matrix for the foundation will suffice for most practical purposes, given that the external and the parametric excitations of offshore wind turbines are dominant in the low-frequency range below 5 Hz.

It is concluded that the coupling between horizontal sliding and rocking must be considered by the lumped-parameter models to avoid significant loss of accuracy. Further, it has been found that the asymptotic behaviour in the high-frequency domain must be based the flexibility of the skirts. Thus, a great difference has been identified between the dynamic stiffness of idealised rigid and more realistic, flexible foundations. Future research will focus on the application of the lumped-parameter models for the analysis soil–structure interaction related to wind turbines.

REFERENCES

Andersen, L. (2002). *Wave propagation in inifinite structures and media*. Ph.D. thesis, Aalborg University, Aalborg, Denmark.

Andersen, L. (2008). Assessment of lumped-parameter models for rigid footings. Computers and Structures, article in press, DOI: 10.1016/j.compstruc.2008.10.007.

Andersen, L. & Jones, C.J.C. (2001). Beasts — a computer program for boundary element analysis of soil and three-dimensional structures. ISVR Technical Memorandum 868, Institute of Sound and Vibration Research, University of Southampton, Southampton, UK.

Andersen, L. & Liingaard, M.A. (2007). Lumped-parameter models for wind-turbine footings on layered ground. In B. Topping (Ed.), *Proceedings of the Eleventh International Conference on Civil, Structural and Environmental Engineering Computing*. Civil-Comp Press, Stirlingshire, United Kingdom.

Bu, S. & Lin, C.H. (1999). Coupled horizontal-rocking impedance functions for embedded square foundations at high frequency factors. *Journal of Earthquake Engineering 3*, 561–587.

Cook, R.D., Malkus, D.S., Plesha, M.E., & Witt, R.J. (2002). *Concepts and Applications of Finite Element Analysis* (4th edition ed.). John Wiley & Sons, Inc., United States of America.

Domínguez, J. (1993). *Boundary elements in dynamics*. Computational Mechanics Publications, Southampton, United Kingdom.

Ibsen, L.B. (2008). Implementation of a new foundations concept for offshore wind farms. In *Proceedings of the 15th Nordic Geotechnical Meeting*, Sandefjord, Norway, pp. 19–33.

Jonkman, J.M. & Buhl, M.L. (2005). Fast user's guide. Technical Report NREL/EL-500-38230, National Renewable Energy Laboratory, Colorado, United States of America.

Liingaard, M. (2006). *Dynamic behaviour of suction caissons*. Ph.D. thesis, Aalborg University, Aalborg, Denmark.

Veletsos, A.S. & Wei, Y.T. (1971). Lateral and rocking vibration of footings. *Journal of the Soil Mechanics and Foundation Engineering Division, ASCE 97*, 1227–1248.

Wolf, J.P. (1994). *Foundation Vibration Analysis Using Simple Physical Models*. Prentice-Hall, Englewood Cliffs, NJ, United States of America.

Wolf, J.P. & Paronesso, A. (1992). Lumped-parameter model for a rigid cylindrical foundation embedded in a soil layer on rigid rock. *Earthquake Engineering and Structural Dynamics 21*, 1021–1038.